

Dynamical Susceptibility in KDP-type Crystals above and below T_c II

Shun-ichi YOSHIDA*, Norihiro IHARA and Koh WADA

Division of Physics, Graduate School of Science, Hokkaido University, Sapporo 060-0810

(Received March 22, 2022)

The path probability method (PPM) in the tetrahedron-cactus approximation is applied to the Slater-Takagi model with dipole-dipole interaction for KH_2PO_4 -type hydrogen-bonded ferroelectric crystals in order to derive a small dip structure in the real part of dynamical susceptibility observed at the transition temperature T_c . The dip structure can be ascribed to finite relaxation times of electric dipole moments responsible for the first order transition with contrast to the critical slowing down in the second order transition. The light scattering intensity which is related to the imaginary part of dynamical susceptibility is also calculated above and below the transition temperature and the obtained central peak structure is consistent with polarization fluctuation modes in Raman scattering experiments.

KEYWORDS: KDP(KH_2PO_4), Slater-Takagi model, PPM(path probability method), dynamical susceptibility, light scattering intensity

1. Introduction

In the previous paper¹⁾(this article is referred to as I henceforth), we have succeeded in calculating the dynamical susceptibility for the Slater-Takagi model²⁾ above and below the transition temperature T_c by making use of the analytical solution for spontaneous polarization in the tetrahedron-cactus approximation of the cluster variation method(CVM).³⁾ This approximation is the basic one in the CVM for taking into account the ice-rule for protons of KDP-type hydrogen bonded ferroelectrics. However, since the Slater-Takagi model always yields the second order phase transition, the dynamical susceptibility at $T = T_c$ almost vanishes as a result of critical slowing down of the most dominant mode governing the transition. This result is different from the experimental data of KDP (KH_2PO_4) which show only a small dip at $T = T_c$ in the real part of dynamical susceptibility versus temperature graph.⁴⁾

It is believed that KDP undergoes the first order transition close to the second order. Senko⁵⁾ phenomenologically introduced the dipole-dipole interaction to the Slater-Takagi model and Silsbee *et al.*⁶⁾ revealed that the phase transition of this model with dipole-dipole interaction changes from the second order to the first order transition according to increase of the strength of dipole-dipole interaction. Based on this model Matsumoto and Ogura⁷⁾ have calculated the light scattering intensity related to the imaginary part of the dynamical susceptibility in the tetrahedron-cactus approximation. However, their calculation seems to be limited to the paraelectric phase. In the present manuscript we would like to show the small dip structure at the transition temperature in the experimental data of the real part of dynamical susceptibility versus temperature for KDP-type crystal. We will also calculate the light scattering intensity below the transition temperature as well as above it. For that purpose we apply the tetrahedron cactus approximation of the PPM (Path Probability Method)⁸⁾ to the Slater-Takagi model with phenomenologically induced dipole-

dipole interaction since we expect that the most dominant mode governing the transition brings about a finite relaxation time at the transition temperature.

2. Formulation

There are N PO_4 tetrahedra and $2N$ protons in KDP-type crystals as shown in Fig. 1. The pseudo-spin Ising Hamiltonian \mathcal{H} for a configuration of $2N$ protons has a form

$$\mathcal{H} = \sum_{\langle ijkl \rangle} \left(\mathcal{H}_0(\sigma_i, \sigma_j, \sigma_k, \sigma_l) - \frac{\mu_d E}{2} (\sigma_i + \sigma_j + \sigma_k + \sigma_l) \right) + \mathcal{H}_{\text{dipole}}, \quad (1)$$

with

$$\begin{aligned} \mathcal{H}_0(\sigma_i, \sigma_j, \sigma_k, \sigma_l) \\ = -V_2(\sigma_i \sigma_j + \sigma_j \sigma_k + \sigma_k \sigma_l + \sigma_l \sigma_i) \\ - V_4 \sigma_i \sigma_j \sigma_k \sigma_l - V_5(\sigma_i \sigma_k + \sigma_j \sigma_l) + C, \end{aligned} \quad (2)$$

and

$$\begin{aligned} \mathcal{H}_{\text{dipole}} = - \sum_{\langle ijkl \rangle} \lambda \mu_d^2 m (\sigma_i + \sigma_j + \sigma_k + \sigma_l) \\ + 2N \lambda \mu_d^2 m^2, \end{aligned} \quad (3)$$

where the sum $\langle ijkl \rangle$ runs over four protons i, j, k, l around each PO_4 tetrahedron in the crystal, μ_d is the magnitude of an electric dipole moment associated with a complex $\text{K-H}_2\text{PO}_4$, E is an external electric field, λ is a parameter representing long range dipolar sum in the phenomenologically introduced dipole-dipole interaction $\mathcal{H}_{\text{dipole}}$ and m is the electric polarization defined by thermal average over \mathcal{H} as

$$m = \langle \sigma_i \rangle = \langle \sigma_j \rangle = \langle \sigma_k \rangle = \langle \sigma_l \rangle, \quad (4)$$

and $2N \lambda \mu_d^2 m^2$ in $\mathcal{H}_{\text{dipole}}$ is taken care of over-counting due to molecular field.

* E-mail: shun1@statphys.sci.hokudai.ac.jp

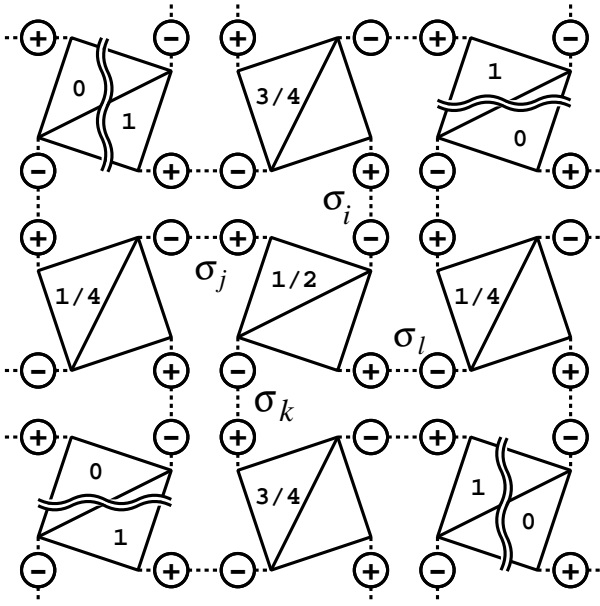


Fig. 1. The projection of atomic arrangement of KDP-type crystals on (001) plane. The variables $\sigma_i, \sigma_j, \sigma_k, \sigma_l$ show the four different pseudo-spins for protons around a PO_4 tetrahedron. The number described in a PO_4 tetrahedron represents a relative height of a PO_4 tetrahedron.

Energy	Proton Configuration	Dipole moment along c -axis	Occurrence Probability
ε_2		0	c_2
ε_1		$+\mu_d$	d_+
		$-\mu_d$	d_-
ε_0		0	c_0
0		$+2\mu_d$	c_+
		$-2\mu_d$	c_-

Slater model¹

Fig. 2. Configuration energy ($\varepsilon_2 > \varepsilon_1 > \varepsilon_0 > 0$), allotted dipole moment along c -axis and occurrence probability of proton configuration around PO_4 tetrahedron.

As is seen in Fig. 1, we use a convention that when the i -th proton is located on the closer site to an O atom at the bottom (top) of the PO_4 tetrahedron along the easy c -axis, the i -th proton takes $\sigma_i = +1(-1)$. The energy parameters V_2, V_4, V_5 and C are connected to the energy parameters in the Slater-Takagi model shown in Fig. 2 as

$$\begin{aligned} V_2 &= \varepsilon_2/8, & V_4 &= -\varepsilon_0/4 + \varepsilon_1/2 - \varepsilon_2/8, \\ V_5 &= \varepsilon_0/4 - \varepsilon_2/8, & C &= \varepsilon_0/4 + \varepsilon_1/2 + \varepsilon_2/8. \end{aligned} \quad (5)$$

As shown in I, we now apply the path probability method (PPM)⁸⁾ in the tetrahedron-cactus approximation to the present system in order to find the time evolution equation of the system with various proton configurations. After some manipulations of the PPM we can make a generating function from which a set of time evolution equations is derived through differentiation of

an interaction parameter set $\mathbf{L} \equiv (L_1, L_2, L_3, L_4, L_5)$. The generating function is given by

$$\mathcal{G}(\mathbf{L}) = \frac{1}{\tau_0} \text{Tr}_i p_1(\sigma_i, t) e^{-2L_1 \sigma_i} \times \left[\frac{\text{Tr}_{jkl} p_4(\sigma_i, \sigma_j, \sigma_k, \sigma_l, t) e^{-\frac{\beta}{2} \Delta_i \mathcal{H}_0(\sigma_i, \sigma_j, \sigma_k, \sigma_l)}}{p_1(\sigma_i, t)} \right]^2,$$

$$\begin{aligned} \Delta_i \mathcal{H}_0(\sigma_i, \sigma_j, \sigma_k, \sigma_l) &= \mathcal{H}_0(-\sigma_i, \sigma_j, \sigma_k, \sigma_l) - \mathcal{H}_0(\sigma_i, \sigma_j, \sigma_k, \sigma_l), \\ L_1 &= \frac{1}{2} (\beta \mu_d E + 2\beta \lambda \mu_d^2 m(t)), \\ L_2 &= \beta V_2, \quad L_3 = \beta V_3, \quad L_4 = \beta V_4, \quad L_5 = \beta V_5, \end{aligned} \quad (6)$$

where Tr_i and Tr_{jkl} denotes a trace operation $\sum_{\sigma_i=\pm 1}$ and $\sum_{\sigma_j, \sigma_k, \sigma_l=\pm 1}$, respectively, $\beta = 1/k_B T$ is the inverse temperature with Boltzmann's constant k_B , $\Delta_i \mathcal{H}_0(\sigma_i, \sigma_j, \sigma_k, \sigma_l)$ defines an energy change under transfer of i -th proton between the double well potential on a hydrogen bond and τ_0 is its microscopic relaxation time of an isolated proton. When $\lambda = 0$, the generating function $\mathcal{G}(\mathbf{L})$ coincides with that of I. Thus, the effect of dipole-dipole interaction modifies only the external electric field E by $E + 2\lambda \mu_d m(t)$. Further, state variables $p_1(\sigma_i, t)$ and $p_4(\sigma_i, \sigma_j, \sigma_k, \sigma_l, t)$ represent, respectively, the probability of finding the site σ_i of a proton in the i -th hydrogen bond at time t and the probability of finding the sites $\sigma_i, \sigma_j, \sigma_k, \sigma_l$ of protons i, j, k, l around a PO_4 tetrahedron at time t . The state variables p_1 and p_4 are given by

$$\begin{aligned} p_1(\sigma_i, t) &= \frac{1}{2} (1 + m(t) \sigma_i), \\ p_4(\sigma_i, \sigma_j, \sigma_k, \sigma_l, t) &= \frac{1}{2^4} \left(1 + \frac{m_1(t)}{4} (\sigma_i + \sigma_j + \sigma_k + \sigma_l) \right. \\ &\quad + \frac{m_2(t)}{4} (\sigma_i \sigma_j + \sigma_j \sigma_k + \sigma_k \sigma_l + \sigma_l \sigma_i) \\ &\quad + \frac{m_3(t)}{4} (\sigma_i \sigma_j \sigma_k + \sigma_j \sigma_k \sigma_l + \sigma_k \sigma_l \sigma_i + \sigma_l \sigma_i \sigma_j) \\ &\quad \left. + m_4(t) \sigma_i \sigma_j \sigma_k \sigma_l + \frac{m_5(t)}{2} (\sigma_i \sigma_k + \sigma_j \sigma_l) \right). \end{aligned} \quad (7)$$

Here let us introduce the Ising spin space vector $\boldsymbol{\sigma}$ around a PO_4 tetrahedron as

$$\boldsymbol{\sigma} = \begin{pmatrix} \sigma_i + \sigma_j + \sigma_k + \sigma_l \\ \sigma_i \sigma_j + \sigma_j \sigma_k + \sigma_k \sigma_l + \sigma_l \sigma_i \\ \sigma_i \sigma_j \sigma_k + \sigma_j \sigma_k \sigma_l + \sigma_k \sigma_l \sigma_i + \sigma_l \sigma_i \sigma_j \\ \sigma_i \sigma_j \sigma_k \sigma_l \\ \sigma_i \sigma_k + \sigma_j \sigma_l \end{pmatrix} \quad (8)$$

Then, in the tetrahedron-cactus approximation of the PPM, the homogeneous state of the present system at time t is found to be described by the five order param-

eters defined by

$$\begin{pmatrix} m_1 \\ m_2 \\ m_3 \\ m_4 \\ m_5 \end{pmatrix} = \begin{pmatrix} \langle \sigma_i + \sigma_j + \sigma_k + \sigma_l \rangle \\ \langle \sigma_i \sigma_j + \sigma_j \sigma_k + \sigma_k \sigma_l + \sigma_l \sigma_i \rangle \\ \langle \sigma_i \sigma_j \sigma_k + \sigma_j \sigma_k \sigma_l + \sigma_k \sigma_l \sigma_i + \sigma_l \sigma_i \sigma_j \rangle \\ \langle \sigma_i \sigma_j \sigma_k \sigma_l \rangle \\ \langle \sigma_i \sigma_k + \sigma_j \sigma_l \rangle \end{pmatrix} \quad (9)$$

where each order parameter represents the correlation of protons i, j, k, l around a PO_4 tetrahedron at time t , $\langle \cdots \rangle_t$ is a thermal average at time t and $m(t) = m_1(t)/4$ is the long range order parameter due to electric polarization per proton. Then a set of kinetic equations for five order parameters is given in a convenient form as

$$\frac{dm_i(t)}{dt} = 4 \lim_{L_3 \rightarrow 0} \frac{\partial \mathcal{G}(\mathbf{L})}{\partial L_i} \quad (i = 1 \sim 5). \quad (10)$$

Here it should be noted that in order to write the above expression an extra interaction term is virtually added to Hamiltonian (2) for technical convenience as

$$\begin{aligned} & \mathcal{H}_0(\sigma_i, \sigma_j, \sigma_k, \sigma_l) \\ & - V_3(\sigma_i \sigma_j \sigma_k + \sigma_j \sigma_k \sigma_l + \sigma_k \sigma_l \sigma_i + \sigma_l \sigma_i \sigma_j) \\ & \rightarrow \mathcal{H}_0(\sigma_i, \sigma_j, \sigma_k, \sigma_l), \end{aligned} \quad (11)$$

and V_3 is, however, put to zero just after differentiation with respect to L_3 in eq.(10).

3. Static Properties

As shown in I, in order to obtain dynamical susceptibility $\chi(\omega)$ as a linear response to an external field E , equilibrium values of order parameters are required at each temperature. Since the equilibrium state is more easily obtained from the cluster variation method (CVM)⁹⁾ rather than from the stationary solution of the time evolution equations(10), we apply the tetrahedron-cactus approximation of the CVM to the present system.¹⁰⁾ The variational free energy G is obtained by

$$G = U - TS, \quad (12)$$

where the internal energy U is given by

$$\frac{U}{N} = -V_2 m_2 - V_4 m_4 - V_5 m_5 - 2\mu_d E m_1 - 2\lambda \mu_d^2 m_1^2, \quad (13)$$

and the entropy S is given by

$$\begin{aligned} \frac{S}{Nk_B} &= \text{Tr}_i [p_1(\sigma_i) \ln p_1(\sigma_i)] \\ &- \text{Tr}_{ijkl} [p_4(\sigma_i, \sigma_j, \sigma_k, \sigma_l) \ln p_4(\sigma_i, \sigma_j, \sigma_k, \sigma_l)]. \end{aligned} \quad (14)$$

Here c_+, c_-, c_0, d_+, d_- and c_2 shown in Fig. 2 are defined through $p_4(\sigma_i, \sigma_j, \sigma_k, \sigma_l)$ as

$$\begin{aligned} c_+ &= \frac{1}{24}(1 + m_1 + m_2 + m_3 + m_4 + m_5), \\ c_- &= \frac{1}{24}(1 - m_1 + m_2 - m_3 + m_4 + m_5), \\ c_0 &= \frac{1}{24}(1 + m_4 - m_5), \\ d_+ &= \frac{1}{24}(1 + m_1/2 - m_3/2 - m_4), \\ d_- &= \frac{1}{24}(1 - m_1/2 + m_3/2 - m_4), \\ c_2 &= \frac{1}{24}(1 - m_2 + m_4 + m_5), \end{aligned} \quad (15)$$

with a normalization condition

$$c_+ + c_- + 4c_0 + 4(d_+ + d_-) + 2c_2 = 1. \quad (16)$$

Since it is sometimes more convenient to use c_+, c_-, c_0, d_+, d_- and c_2 instead of $m_1 \sim m_5$ especially in thermostatic discussions, we rewrite the variational free energy in terms of c_+, c_-, c_0, d_+, d_- and c_2 as

$$\begin{aligned} \frac{G}{N} &= 4\varepsilon_0 c_0 + 4\varepsilon_1(d_+ + d_-) + 2\varepsilon_2 c_2 \\ &- 2\lambda \mu_d^2 (p_+ - p_-)^2 - 2\mu_d E (p_+ - p_-) \\ &- k_B T (2p_+ \ln p_+ + 2p_- \ln p_- - c_+ \ln c_+ - c_- \ln c_- \\ &- 4c_0 \ln c_0 - 4d_+ \ln d_+ - 4d_- \ln d_- - 2c_2 \ln c_2) \\ &+ s(1 - (c_+ + c_- + 4c_0 + 4(d_+ + d_-) + 2c_2)), \end{aligned} \quad (17)$$

with

$$\begin{aligned} p_1(+1) &\equiv p_+ = c_+ + 2c_0 + 3d_+ + d_- + c_2, \\ p_1(-1) &\equiv p_- = c_- + 2c_0 + d_+ + 3d_- + c_2, \end{aligned} \quad (18)$$

where s is the Lagrange multiplier to make all the state variables c_+, c_-, c_0, d_+, d_- and c_2 independent. With $\lambda = 0$ this expression of the free energy reduces to that of Ishibashi.³⁾ Under a uniform electric field the thermal equilibrium state is obtained from the minimum condition of the free energy: $\partial G / \partial c_+ = \partial G / \partial c_- = \partial G / \partial c_0 = \partial G / \partial d_+ = \partial G / \partial d_- = \partial G / \partial c_2 = 0$ as

$$\begin{aligned} c_0 &= \frac{\eta_0}{4\eta_0 + 2\eta_2 + ((hA)^2 + (hA)^{-2}) + 4\eta_1(hA + (hA)^{-1})}, \\ c_+ &= (hA)^2 \left(\frac{c_0}{\eta_0} \right), \quad c_- = (hA)^{-2} \left(\frac{c_0}{\eta_0} \right), \quad c_2 = \eta_2 \left(\frac{c_0}{\eta_0} \right), \\ d_+ &= (hA)\eta_1 \left(\frac{c_0}{\eta_0} \right), \quad d_- = (hA)^{-1}\eta_1 \left(\frac{c_0}{\eta_0} \right) \end{aligned} \quad (19)$$

where

$$\begin{aligned} \eta_i &= \exp(-\beta\varepsilon_i), \quad (i = 0, 1, 2) \\ A &= \sqrt{\frac{1+m}{1-m}} \exp(2Dm), \quad (D = \beta\lambda\mu_d^2) \\ h &= \exp(\beta\mu_d E). \end{aligned} \quad (20)$$

Further, the polarization m is determined by the relation

$$m = p_+ - p_- = c_+ - c_- + 2(d_+ - d_-) \quad (21)$$

In order to investigate properties of the phase transition we make the Landau-type variational free energy $G(m, E, T)$ as a function of the electric polarization m by substituting (19) into eq.(17):

$$\begin{aligned} &\frac{G(m, E, T)}{Nk_B T} \\ &= 2Dm^2 - \ln \frac{1-m^2}{4} \\ &\quad - \ln((A^2 + A^{-2}) + 4\eta_0 + 4\eta_1(A + A^{-1}) + 2\eta_2) \end{aligned} \quad (22)$$

It is noteworthy that $G(m, E, T)$ has a property $\partial G(m, E, T)/\partial m = 0$ at the thermal equilibrium state. Now, we expand $G(m, E, T)$ in terms of order parameter m up to the 4-th order:

$$\begin{aligned} \frac{G(m, E, T)}{Nk_B T} &= -\ln \frac{\Gamma}{2} + \frac{1}{2}A_2(T)m^2 + \frac{1}{4}A_4(T)m^4 + \dots \\ &\quad - \frac{4\mu_d(1+2D)(1+\eta_1)}{\Gamma k_B T} m E \end{aligned} \quad (23)$$

where Γ , $A_2(T)$ and $A_4(T)$ are given by

$$\begin{aligned} \Gamma &= 1 + 2\eta_0 + 4\eta_1 + \eta_2, \\ A_2(T) &= 2(1+2D) \left(1 - \frac{2(1+2D)(1+\eta_1)}{\Gamma} \right), \\ A_4(T) &= \frac{A_2(T)}{1-2D} + \frac{2(1+2D)}{\Gamma^2} \left(4(1+2D)^3(1+\eta_1)^2 \right. \\ &\quad \left. - \frac{\Gamma}{3}(2(1+\eta_1) + (4+\eta_1)(1+2D)^3) \right) \end{aligned} \quad (24)$$

From the view point of Landau's phase transition theory the order of the phase transition is classified as follows. (i) The phase transition undergoes the second order transition at T_0 if $A_2(T_0) = 0$ and $A_4(T_0) > 0$. (ii) The phase transition undergoes the first order phase transition at $T_c(> T_0)$ if $A_2(T_0) = 0$ and $A_4(T_0) < 0$. The boundary between the first and the second order is called the tricritical point $T_t(= T_0)$ when $A_2(T_0) = 0$ and $A_4(T_0) = 0$. Based on eq.(24) we can get the phase diagram in Fig. 3. Since an increase of the phenomenologically introduced dipole-dipole interaction strengths the mechanical ferroelectric order effect, the ferroelectric transition becomes possible before the system comes to an instability point when the temperature is decreased. This is the reason why the dipole-dipole interaction induces the first order transition instead of the second order transition. As is

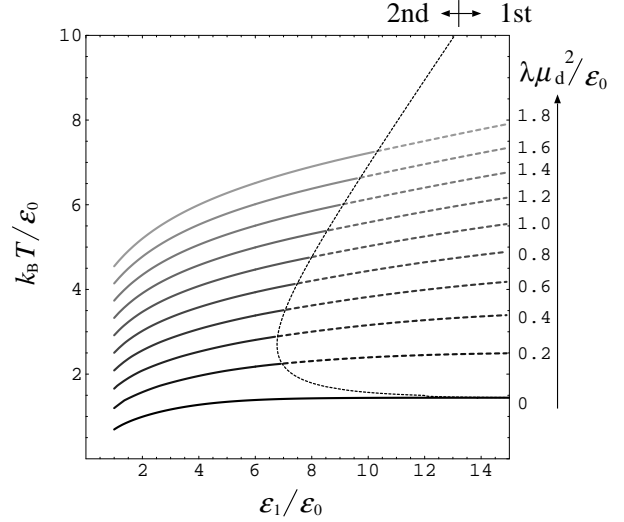


Fig. 3. The phase diagram of the Slater-Takagi model with dipole-dipole interaction. The solid line stands for the second order phase transition and the dotted one stands for the first order phase transition.

shown in Fig.3, with $\varepsilon_1/\varepsilon_0$ being decreased for each λ , the transition temperature is decreased because more easily thermal excitation of protons favors the paraelectric phase. When $A_2(T_0) = 0$ for $\lambda\mu_d^2/\varepsilon_0 = 0$ (Slater-Takagi model), $A_4(T_0) = \eta_1/(1+\eta_1)$ is positive definite. That is, the Slater-Takagi model always undergoes the second order phase transition. Especially, in the Slater model ($\lambda = 0, \varepsilon_0 > 0, \varepsilon_2 > \varepsilon_1 \rightarrow \infty$) the phase transition takes place at the tricritical point. Therefore, it is sometimes said that the transition derived by the Slater theory has the nature of both the first and the second order phase transitions. On the other hand, as is seen in eq.(24) the first order phase transition is caused by the finite value $\lambda\mu_d^2/\varepsilon_0 > 0$. As $\lambda\mu_d^2/\varepsilon_0$ is increased, the first order transition region becomes larger and the transition temperature T_c is also increased. However, when the dipolar term becomes dominant, the second order transition region again widens because of the phenomenologically induced dipolar interaction.

In order to fix the values of unknown parameters we utilize the experimental data on the temperature dependence of spontaneous polarization¹²⁾ and choose the parameters such as $\varepsilon_1/\varepsilon_0 = 9.48, \varepsilon_2/\varepsilon_0 = 36.92, \lambda\mu_d^2/\varepsilon_0 = 1.095$ in the case of first order phase transition. This parameter set shows a ratio of spontaneous polarization jump to saturated spontaneous polarization about 0.4. As a comparison with the case of the first order phase transition we choose the same parameter set as $\varepsilon_1/\varepsilon_0 = 9.48, \varepsilon_2/\varepsilon_0 = 36.92$ except $\lambda\mu_d^2/\varepsilon_0 = 0$ in the case of second order phase transition. In the following this set of parameters is used in the present calculations.

Though without dipole-dipole interaction term $\lambda = 0$ we could study the static properties analytically thanks to explicit expression of spontaneous polarization,³⁾ with $\lambda \neq 0$ we cannot obtain analytical spontaneous polarization anymore. However, we can deal with these simultaneous equations numerically by making use of the natural iteration method (NIM)¹³⁾ for the CVM. Through

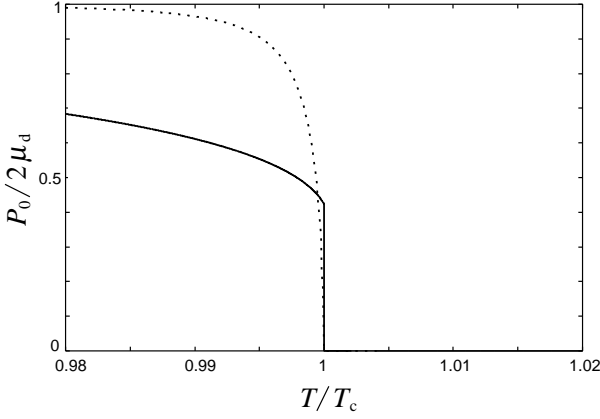


Fig. 4. The temperature dependence of spontaneous polarization. The solid line (first order) and dotted one (second order) are shown. In the first order case the spontaneous polarization jump at $T = T_c$ is about 0.4.

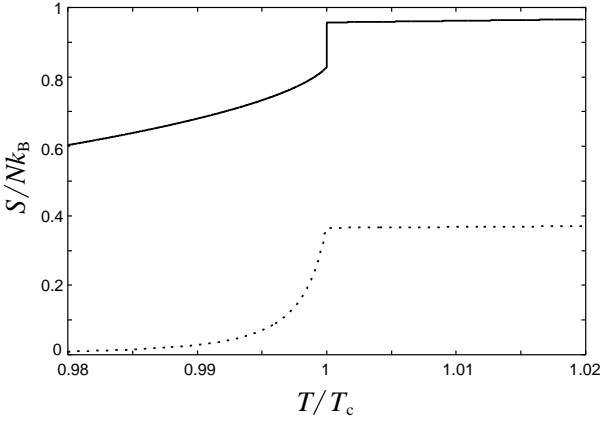


Fig. 5. The entropy versus temperature. The solid line (first order) and dotted one (second order) are shown.

the NIM calculation we can obtain the physical quantities such as the spontaneous polarization $P_0 \equiv 2\mu_d m_0$ per PO_4 and the entropy S for each case of the first and the second order transition (Fig. 4 and Fig. 5). These numerical results will be used to calculate dynamical susceptibility.

The static uniform susceptibility χ_{stat} of the system is also obtained as the linear response Δm from m_0 induced by a uniform field E from the equation of state (21) as

$$\chi_{\text{stat}} \equiv \frac{2N\mu_d \Delta m}{E} = \frac{2N\mu_d^2}{k_B T} \frac{1}{X^{-1} - \left(\frac{1}{1-m_0^2} + 2D \right)}, \quad (25)$$

with

$$\begin{aligned} A_0 &= \sqrt{\frac{1+m_0}{1-m_0}} \exp(2Dm_0), \\ \alpha_0 &= (A_0^2 + A_0^{-2} + 4\eta_0 + 4\eta_1(A_0 + A_0^{-1}) + 2\eta_2)^{-1}, \\ X &= 2\alpha_0(A_0^2 + A_0^{-2} + (A_0 + A_0^{-1})\eta_1) - 2m_0^2, \end{aligned} \quad (26)$$

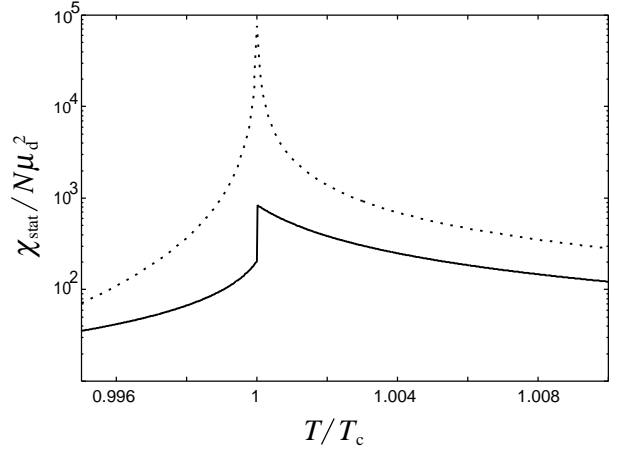


Fig. 6. The uniform susceptibility versus temperature. The solid line (first order) and dotted one (second order) are shown.

where m_0 is given from eq.(21) by

$$m_0 = \alpha_0(A_0^2 - A_0^{-2} + 2\eta_1(A_0 - A_0^{-1})). \quad (27)$$

When $D = 0$, this result reduces to our previous result for the Slater-Takagi model without dipole-dipole interaction.¹⁾ The numerical result of uniform susceptibility χ_{stat} is shown in Fig. 6.

4. Dynamical Susceptibility

By making use of the numerical results obtained in the previous section, let us calculate dynamical susceptibility in this section. When an external electric field $E(t) = E \exp(i\omega t)$ is applied, we assume that

$$m_i(t) = m_i^0 + \chi_i(\omega) E \exp(i\omega t) \quad (i = 1 \sim 5) \quad (28)$$

where the required dynamical susceptibility is given by $\chi(\omega) = \mu_d \chi_1(\omega)/4$ since it is the response of electric polarization to a weak electric field, and m_i^0 's are equilibrium order parameters in the absence of an external field. It should be noted that $m_i^0 (i = 1 \sim 5)$ are obtained numerically by the NIM calculation. By substituting these relations (28) into (10) we get the following algebraic equations up to the linear order to external field:

$$(i\omega\tau_0 I + M) \chi(\omega) = \mathbf{b}, \quad (29)$$

where $\chi(\omega) = (\chi_1(\omega) \chi_2(\omega) \chi_3(\omega) \chi_4(\omega) \chi_5(\omega))^t$ and I is the 5×5 unit matrix. Since the elements of 5×5 matrix M and a 5×1 column vector \mathbf{b} are a little lengthy quantities expressed in terms of only η_0, η_1, η_2 and D , we omit them here. After numerical calculations by the Gaussian elimination method for a fixed $\omega\tau_0$ we get the dynamical susceptibility over all the temperature region. With the relaxation times $\tau_i (i = 1 \sim 5)$ and the intensity coefficients χ^i , the dynamical susceptibility per proton $\chi(\omega)$ can be written as

$$\chi(\omega) = \frac{\mu_d}{4} \chi_1(\omega) = \sum_{i=1}^5 \frac{\chi^i}{1 + i\omega\tau_i}, \quad (30)$$

where the five relaxation times τ_i are obtained by a diagonalization of M in terms of a matrix U as

$$(UMU^{-1})_{ij} = \frac{\tau_0}{\tau_i} \delta_{ij}, \quad (\delta_{ij} : \text{Kronecker's delta}) \quad (31)$$

and the intensity coefficients χ^i are given by

$$\chi^i = \frac{\mu_d}{4\tau_0} \tau_i \sum_{j=1}^5 (U^{-1})_{1i} U_{ij} b_j. \quad (32)$$

Especially in the paraelectric phase we note that, under the inversion of an external field E , the order parameters m_1 and m_3 are changed into $-m_1$ and $-m_3$, respectively, while m_2, m_4 and m_5 are invariant. Accordingly, m_1 and m_3 are long range order parameters responding linearly to external field E , while m_2, m_4 and m_5 are short range order parameters responding quadratically to the field. Thus in the paraelectric phase eq. (29) is reduced to a closed algebraic equation in m_1 and m_3 space and as a result the dynamical susceptibility (30) can be written down as

$$\chi(\omega) = \frac{\chi^1}{1 + i\omega\tau_+} + \frac{\chi^3}{1 + i\omega\tau_-}, \quad (33)$$

where

$$\begin{aligned} \tau_{\pm} &= \frac{2}{p \mp \sqrt{p^2 - 4q}} \quad (\tau_+ = \tau_1, \tau_- = \tau_3), \\ p &= 2 \left(1 + \frac{2\eta_0 + 4\sqrt{\eta_0\eta_2} + 2\eta_1(2\sqrt{\eta_0} + \sqrt{\eta_2})}{\Gamma} - 2K^2(1 + 2D) \right), \\ q &= 8K^2(2\sqrt{\eta_0} + \sqrt{\eta_2}) \left(1 - \frac{2(1 + 2D)(1 + \eta_1)}{\Gamma} \right), \\ \chi^1 &= \frac{8\beta\mu_d^2 K^2 \tau_+ \tau_-}{(\tau_+ - \tau_-)\tau_0} \left(\frac{8(1 + \eta_1)(2\sqrt{\eta_0} + \sqrt{\eta_2})}{\Gamma} \frac{\tau_+}{\tau_0} - 1 \right), \\ \chi^3 &= \frac{8\beta\mu_d^2 K^2 \tau_+ \tau_-}{(\tau_+ - \tau_-)\tau_0} \left(1 - \frac{8(1 + \eta_1)(2\sqrt{\eta_0} + \sqrt{\eta_2})}{\Gamma} \frac{\tau_-}{\tau_0} \right), \end{aligned} \quad (34)$$

with

$$K = \frac{(1 + 2\sqrt{\eta_0} + \sqrt{\eta_2})\sqrt{\eta_1}}{\Gamma}. \quad (35)$$

Next, we plot the real and imaginary part of dynamical susceptibility over all the temperature region in the first order transition in Fig. 7 and Fig. 8. We see a small dip in the real part of $\chi(\omega)$ (Fig. 7) consistent with the experiments.⁴⁾ We notice from Fig. 9 and Fig. 10 that one of the five modes overwhelms other four modes in relaxation time τ_i and intensity coefficient χ^i , though any relaxation time τ_i is finite at $T = T_c$ in the first order phase transition. That is the reason why the small dip structure appears around the transition temperature in the real part of the dynamical susceptibility. On the other hand, as shown in I, in the Slater-Takagi model the phase transition always becomes the second order and the most dominant mode shows a critical slowing down which leads to the vanishing of the real part of dynamical susceptibility at the transition temperature.

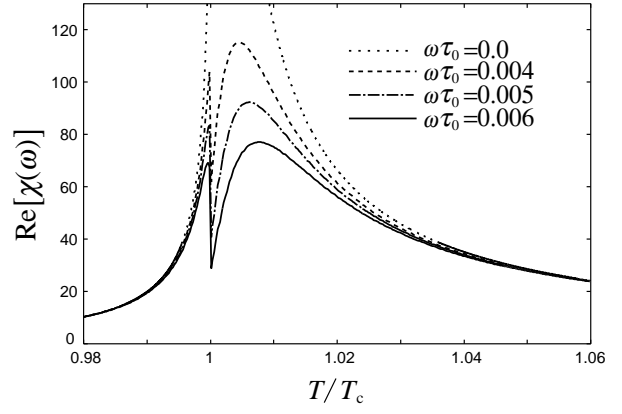


Fig. 7. The real part of dynamical susceptibility in the case of first order phase transition.

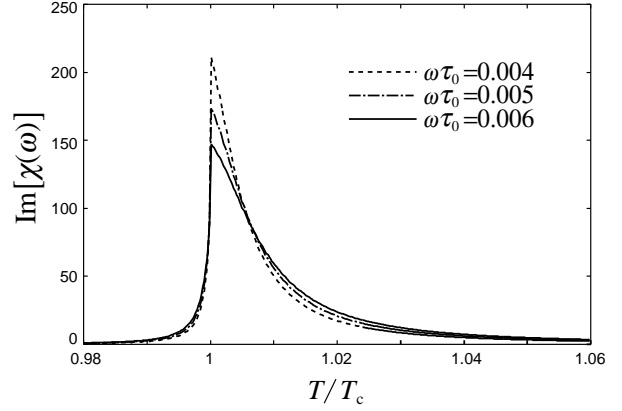


Fig. 8. The imaginary part of dynamical susceptibility in the case of first order phase transition.

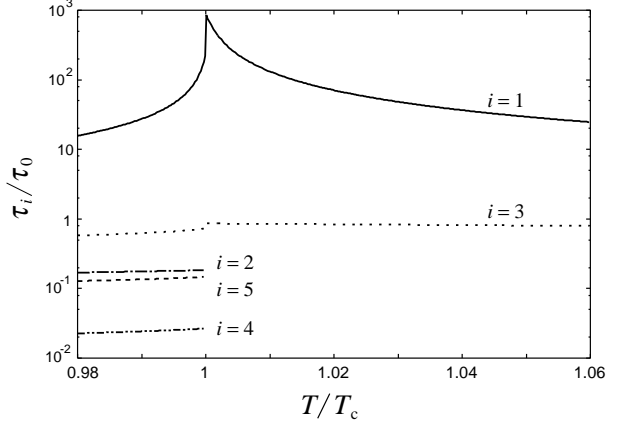


Fig. 9. The five relaxation times versus temperature in the case of first order phase transition. In the paraelectric phase τ_2, τ_4, τ_5 are omitted because any contribution to $\chi(\omega)$ from them do not exist.

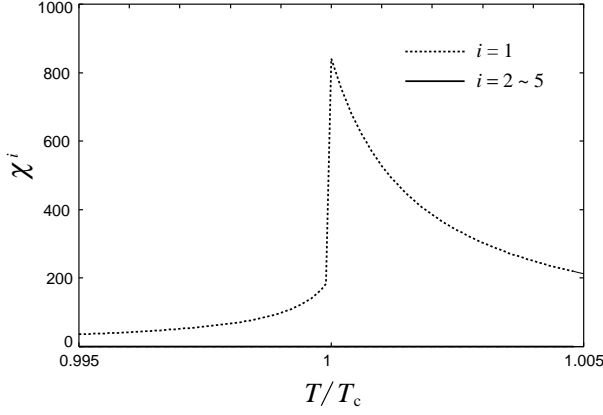


Fig. 10. The five intensities versus temperature in the case of first order phase transition. One of the intensities χ^1 becomes dominant and $\chi^2 \sim \chi^5$ have almost zero value in comparison with χ^1 over all temperature region.

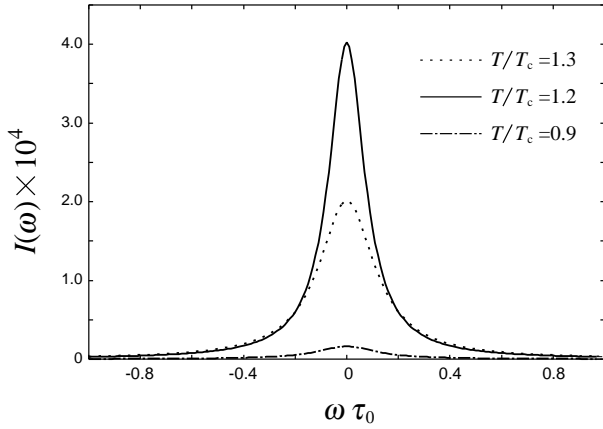


Fig. 11. The frequency dependence of light scattering intensity in the case of first order phase transition.

The imaginary part of dynamical susceptibility is also in qualitative agreement with the experiments.⁴⁾

5. Light Scattering Intensity

Let us calculate the light scattering intensity assuming the first order transition with the same previous set of parameters and compare it with the experimental results. The light scattering intensity $I(\omega)$ is expressed in terms of the imaginary part of $\chi(\omega)$ in the high temperature approximation as

$$I(\omega) \propto \frac{\text{Im}[\chi(\omega)]}{\omega}. \quad (36)$$

The numerical results of $I(\omega)$ are shown in Fig. 11. When the transition temperature is approached from high temperature side above T_c , the height of a peak increases and the width of the peak decreases around $\omega = 0$.⁷⁾ However, since it is assumed to be the first order transition, the height of the peak becomes the largest at the transition temperature but still finite. Moreover, as the temperature is decreased across T_c , the height of the peak around $\omega = 0$ is decreased drastically. The central mode at $\omega = 0$ is caused by the dipolar fluctuations

of relaxation modes in the present model. Further, since from the imaginary part of eq.(30) it is easily obtained as

$$\int_{-\infty}^{\infty} I(\omega) d\omega \propto \int_{-\infty}^{\infty} d\omega \sum_i \frac{\chi^i \tau_i}{1 + (\omega \tau_i)^2} = \pi \sum_{i=1}^5 \chi^i \quad (37)$$

these behaviors are easily understood as follows. Since the total integral value of scattering intensity over ω is proportional to the sum of intensity of relaxation modes at each temperature T , the largest intensity over ω is reached at the transition temperature T_c but does not diverge in the present first order transition. These behaviors agree qualitatively with the experimental data.¹¹⁾

6. Conclusions and Discussions

In order to explain a small dip structure around the ferroelectric transition temperature in the real part of dynamical susceptibility of KDP crystal observed in the experiment, we extend our previous calculation in the Slater-Takagi model to the Slater-Takagi model with phenomenologically introduced dipole-dipole interaction. We applied the path probability method (PPM) to the Slater-Takagi model with dipole-dipole interaction in the tetragonal cactus approximation which can take care of the ice rule characteristic of KDP crystal. With the dipole-dipole interaction being increased, the phase transition changes from the second order into the first order transition. Further, in the present model the phase transition shows the order-disorder transition of proton configurations. We see the dynamical fluctuations of electric polarization modes due to proton configuration in the dynamical susceptibility which is expressed in terms of relaxation times of the electric polarizations with intensity of each mode. The Slater-Takagi model always induces the second order transition and shows a critical slowing down as to relaxation time of the relevant mode. Then the system can not follow the external electric field with finite frequency at the transition temperature T_c due to the critical slowing down. This is the reason why the real part of the dynamical susceptibility gives zero at the critical temperature T_c . On the other hand, the Slater-Takagi model with the appropriate dipole-dipole interaction undergoes the first order transition and the relaxation time of each mode becomes finite. Thus the system can manage to follow the frequency dependent external field, though the relaxation time of relevant mode is relatively long because of the first order transition close to the second order transition of KDP. This fact explains why the dip structure is observed around the transition temperature in the experiment of the real part of dynamical susceptibility. We also calculated the light scattering intensity utilizing the imaginary part of the present dynamical susceptibility. Since our model deals with relaxation modes in the order-disorder transition, we obtain only the central peak structure around $\omega = 0$. This peak structure increases toward the transition temperature, though the height of the peak does not diverges even the transition temperature in the present first order transition. This behavior is in good agreement with the data

of Tominaga *et al.*¹¹⁾

Finally we should note that all our calculations show not quantitative but qualitatively good agreements with experiments which are ascribed to the Slater-Takagi model with phenomenologically introduced dipole-dipole interaction.

- 1) K. Wada, S. Yoshida and N. Ihara: J. Phys. Soc. Jpn. **70** (2001) 1019.
- 2) K. Yoshimitsu and T. Matsubara: Suppl. Prog. Theor. Phys.(Kyoto) (1968) 109.
- 3) Y. Ishibashi: J. Phys. Soc. Jpn. **56** (1987) 2089.
- 4) G. V. Kozlov, S. P. Lebedev, A. A. Minaev, A. A. Volkov and E. V. Monia: Ferroelectrics **21** (1978) 373.
- 5) M. E. Senko: Phys. Rev. **121** (1961) 1599.
- 6) H. B. Silsbee, E. A. Uehling and V. H. Schmidt: Phys. Rev. **133** (1964) A165.
- 7) Y. Matsumoto and K. Ogura: J. Phys. Soc. Jpn. **62** (1993) 3519.
- 8) R. Kikuchi: Prog. Theo. Phys. Suppl. **35** (1966) 1.
- 9) R. Kikuchi: Phys. Rev. **81** (1951) 988.
- 10) N. Ihara, S. Yoshida and K. Wada: J. Phys. Soc. Jpn. **70** (2001) 2550.
- 11) Y. Tominaga, H. Urabe and M. Tokunaga: Solid State Commun. **48** (1983) 265.
- 12) J. Benepe and W. Reese: Phys. Rev. B **3** (1971) 3032.
- 13) R. Kikuchi: J. Chem. Phys. **60** (1974) 1071.